Chen W, Huo D, Teng X, Sun Y.

Surface generation modelling for micro end milling considering the minimum chip thickness and tool runout.

***Procedia CIRP* 2017, 58, 364-369.**

Available online at www.sciencedirect.com

ScienceDirect

Procedia CIRP 58 (2017) 364 – 369

www.elsevier.com/locate/procedia

16th CIRP Conference on Modelling of Machining Operations

Surface generation modelling for micro end milling considering the minimum chip thickness and tool runout

Wanqun Chen[a,b], Dehong Huo[a,*], Xiangyu Teng[a], Yazhou Sun[b]

[a]School of Mechanical and Systems Engineering, Newcastle University, Newcastle upon Tyne, NE1 7RU, UK
[b]Center for Precision Engineering, Harbin Institute of Technology, Harbin, 150001, People's Republic of China

* Corresponding author. Tel.: 44 (0) 191 208 6230; fax: 44 (0) 191 208 6230. E-mail address: dehong.huo@newcastle.ac.uk

Abstract

Surface roughness is considered as one of the significant factors on the quality and functionality of micro components. Considering that in micro milling feed per tooth and uncut chip thickness are very small compared to those in conventional milling, it is necessary to study surface generation precisely in micro scale. This paper proposes a surface generation model for micro-end-milling process, where the effect of the minimum chip thickness (MCT) and tool runout are considered. The MCT values were determined through finite element simulations for AISI 1045 steel, and the magnitude of the tool runout in machining rotational speed was obtained by displacement measurement using capacitive sensors. Based on the proposed model, the influence of the tool runout, MCT as well as the tool geometric parameters on the surface generation was studied. Finally, simulation results were compared with experimental data and a good agreement was obtained.

Peer-review under responsibility of the scientific committee of The 16th CIRP Conference on Modelling of Machining Operations

Keywords: Micro milling; surface generation; modelling; tool runout; minimum chip thickness;

1 Introduction

Micro components are widely in demand in the fields such as electronics, telecommunications, medicine, bioengineering, and optics, which has encouraged the development of micro manufacturing processes [1-4]. Micro milling is recognised as one of the most versatile micro manufacturing processes [5], due to its high applicability for wide workpiece material, capability of producing 3D geometries with complex shape, excellent dimensional accuracy, high efficiency, low cost and environmental friendliness [6-9]. The size of micro features produced by micro milling are normally at the order of several tens to several hundreds of microns, which makes the subsequent finishing processes, e.g. grinding or polishing, expensive or even impossible. Producing high quality surface finishing directly from micro milling to meet certain stringent specification without subsequent processes has become a pressing task. Numerous research has been focused on the study of surface quality in micro milling in recent years. Oliaei and Karpat [10] investigated the influence of machining parameters on the surface roughness of stainless steel machining. Bissacco et al. [11] studied the size effects on surface generation by ball nose and flat end micro milling of hardened tool steel, and the effects of the increased ratio between cutting edge radius and chip thickness have been observed. Saklakoglu and Kasman [12] used regression analysis to develop a mathematical model and determine the effect of process parameters on the surface roughness and milling depth. Sun et at. [13] studied the influence of the feedrate on the surface roughness considering the minimum chip thickness. Vogler et al. [14] proposed a surface generation model to predict the surface roughness for the slot milling based on the minimum chip thickness concept. Li et al. [15] proposed a trajectory-based surface roughness model for micro end milling by considering the minimum chip thickness, micro tool geometry and process parameters. Based on this model, a surface roughness model with tool wear effect was developed by taking the material removal volume

Peer-review under responsibility of the scientific committee of The 16th CIRP Conference on Modelling of Machining Operations
doi:10.1016/j.procir.2017.03.237

and cutting velocity into account and was experimentally validated.

Previous research studied the influence of cutting tool geometry, machining parameters, tool wear and MCT on the surface generation in micro milling. However, spindle or tool runout has been ignored, even though tool runout presents an imperative impact on the surface generation due to the fact that in micro milling the magnitude of tool runout is comparable with the feed per tooth. In this paper, a surface generation model has been established taking account of both tool runout and MCT.

2 Micro cutting tool geometry and spindle runout test

The micro machining system used in this paper is a precision three axis meso-scale milling machine tool (Nanowave MTS5R) which is equipped with a precision high speed spindle with 6,000-80,000 rpm speed range. 0.5 mm diameter two flute tungsten carbide micro end mills were used in the simulation and experiments.

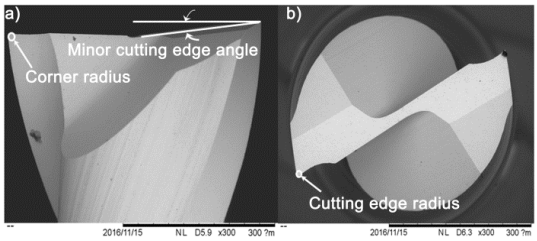

Fig. 1 SEM images of the micro cutter tool used in the simulation and experiment. a) side view; b) top view.

In order to obtain the geometry parameters, the micro end mills were examined by SEM prior to machining experiments. Fig.1 shows the side view and top view of the micro cutting tool. The geometrical parameters of the micro cutting tool are shown in Table 1.

Table 1 Parameters of the micro cutting tool

Parameter	Value
Cutting diameter, D	0.5 mm
Number of flutes, N	2
Cutting edge radius, r_e	3 µm
Minor cutting edge angle, k'_r	5°
Corner radius, r_ε	5µm

Tool runout can be considered as the total amount of inaccuracy of tool manufacturing errors and spindle/tool alignment errors. Different to conventional milling, the ratio of tool runout to tool diameter cannot be neglected in micro milling, thus it considered to be a significant factor during the machining process [16]. To obtain the tool runout in machining rotational speed, a runout test was carried out using a modular capacitive sensor system (capaNCDT 6200, Micro-epsilon) and a capacitive sensor (CS005, Micro-epsilon) with 1nm dynamic resolution and 50 µm measuring range is used. As shown in the schematic in Fig.2, the spindle runout in radial direction was measured on the cylindrical part of the tool.

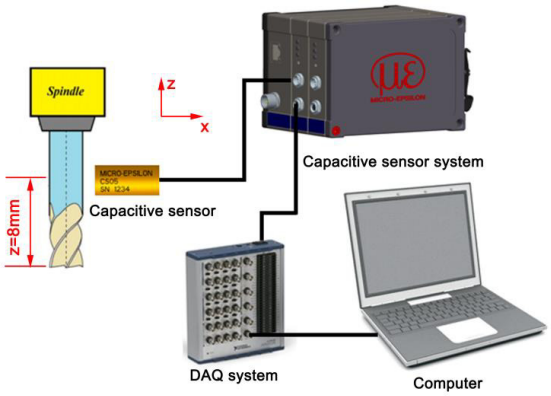

Fig.2 Schematic of the tool runout test

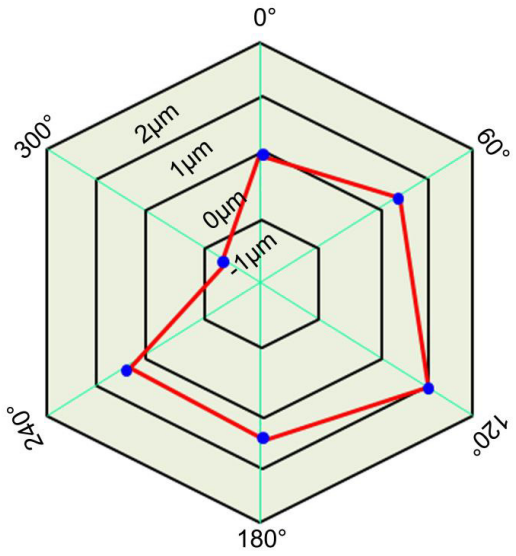

Fig.3 Measured tool run-out offset

Fig. 3 shows the run-out magnitudes and the related run-out angles in a given revolution (40,000 rpm) at z=8mm, which is measured from the tool tip as shown in Fig.2. The tool centre set as the coordinate origin of the tool coordinate system, and the position which parallel to Y axial is set as the 0°. Six angle positions are recorded per revolution at z=8 mm. It can be seen that the maximum measured offset distance and the corresponding location angle, are 1 µm and 120°, respectively.

3 Minimum chip thickness simulation

Due to the difficulties in measuring MCT experimentally, a finite element (FE) model was established using commercial package, ABAQUS/Explicit, to predict the minimum chip thickness. The parameters of the micro cutting tool used in the

FE model are listed in Table 1. AISI 1045 steel was chosen as the workpiece material due to its popularity in plastic injection molding industry. The nonlinear temperature and strain rate sensitive Johnson-Cook (JC) material model was used to describe the material behaviour of the workpiece.

The primary equation of the JC model is

$$\sigma_y = \left[A + B\left(\varepsilon_p\right)^n\right]\left[1 + C ln\left(\dot{\varepsilon}_p^*\right)\right]\left[1 - (T^*)^m\right] \quad (1)$$

where

$$\dot{\varepsilon}_p^* = \frac{\dot{\varepsilon}_p}{\dot{\varepsilon}_{p0}}, T^* = \frac{T - T_0}{T_m - T_0}$$

Here, ε_p is the effective plastic strain, $\dot{\varepsilon}_p$ and $\dot{\varepsilon}_{p0}$ are the plastic strain rate and effective plastic strain rate used for calibration of the model respectively, T and T_0 are the current and reference temperatures respectively.

The parameters A, B, n, C, m, T_m along with other parameters are defined in Table 2 and their values are extracted from Ref.[17].

Table 2 Mechanical properties and parameters for AISI 1045 steel

Properties and parameters	Notation	Value
Density	ρ	7800 kgm^{-3}
Thermal conductivity	K	38 Wm^{-1}K^{-1}
Specific heat	C	420 JKg^{-1}K^{-1}
Tayor-Qulnney coefficient	β	0.9
Initial yield stress	A	553 MPa
Hardening modulus	B	600 MPa
Strain rate dependency coefficient	C	0.0134
Work-hardening exponent	n	0.234
Thermal softening coefficient	m	1
The reference stain rate	$\dot{\varepsilon}_{p0}$	1s^{-1}
Room temperature	T_0	300 K
Melting temperature	T_m	1733 K

In the FE model shown in Fig.4, a half radial immersion up milling was simulated. With the increase of the tool immersion angle θ, the instantaneous uncut chip thickness, h_c, is increased, and it can be found that there chip is not observed when the h_c is less than 0.2 r_e (r_e is the cutting edge radius), while chip forms when the h_c reachs to 0.3 r_e. Based on the FEA results, minimum chip thickness h_{min} is proposed to be 0.25r_e (0.75μm) for AISI 1045 steel when cutter edge radius is 3μm and rake angle is 5°. The results are consistent with the previous study on the minimum chip thickness reported in literature,namely, around 0.05~0.4 times of the cutting edge radius [18-22].

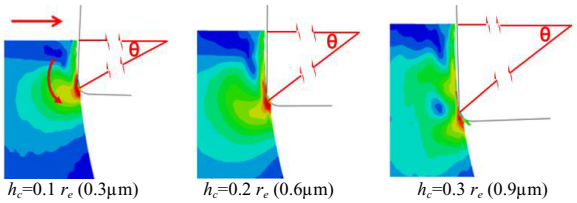

Fig.4 Minimum chip thickness prediction by FE simulation

4 Surface generation modelling of micro milling

4.1 Cutter profile modelling

The surface generation model is established based on the geometry of the micro cutting tool, the tool runout and the MCT. As shown in Fig.5, the milling tool rotates around y-axis and translates along the feed direction (x-axis). In end milling, the workpiece material that comes in contact with the tool cutting edges is removed by the tool. After machining, the workpiece surface is shaped by the tool profile without considering the elastic recovery of machined surface. Therefore, modelling the geometry of the cutting edges along with its kinematics is essential in determining feed marks generated by the individual tooth on the machined surface. The coordinate setting and the end cutting edge geometry of the studied micro-endmill are shown in Fig.5.

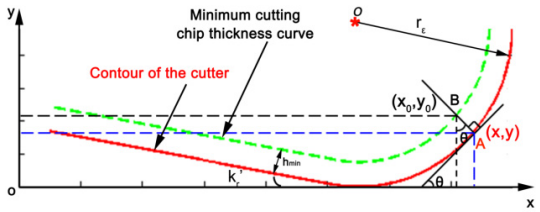

Fig.5 The micro cutter profile and its corresponding minimum chip thickness curve

Fig. 5 shows that the end cutting edge profile of the tool consists of both linear curved segments. The linear segment is inclined with a rake angle, k_r'. This concavity angle provides less contact length and hence reduce friction between the tool and workpiece and at the same time influences the shape of the surface profile of the machined floor surface. The curved segment represents the radius at the tool tip which is the most significant parameter of this geometric model which dominates surface generation in the micro end milling process. The cutter profile (x, y) representing the end cutting edge and the corner radius of the tool can be expressed as:

$$y = \begin{cases} \sqrt{r_\varepsilon^2 - x^2}; & r_\varepsilon \geq x > -r_\varepsilon \sin(k_r') \\ r_\varepsilon \cos(k_r') + \left(x + r_\varepsilon \sin(k_r')\right)\tan(k_r'); & x \leq -r_\varepsilon \sin(k_r') \end{cases} \quad (2)$$

where r_ε denotes the corner radius of the tool and k_r' denotes the rake angle;

Let the coordinate of any point on the cutter profile curves A to be (x, y), the slope of the tangent line through this point is noted as k; The incline between the tangent and the positive x-axis is noted as θ; Thus, the point (x_0, y_0) on the minimum cutting thickness curve B which corresponds to the point $A(x, y)$ on the contour of a micro milling tool, can be given as

$$\begin{cases} x_0 = x - h_{min} sin\theta \\ y_0 = y + h_{min} cos\theta \end{cases} \quad (3)$$

where $\theta = atan(k)$

In the centerline of the machined slot, the radial runout can be simplified as

$$rr_{xi} = rr \cdot (-1)^{i+1} \quad (4)$$

where: rr_{xi} is the x component of the radial runout, μm
rr is the radial runout amplitude, μm
i is the index of the flutes

When considering the radial runout, the cutter profile and the MCT profile moving along the feed direction can be described as $f_z * i + rr_{xi}$. Where f_z is feed per tooth.

Surface generation simulation was carried out at the centerline of slot machining, and the simulation results without and with the tool runout are compared in the next section. The influences of the feed per tooth on the surface generation considering the MCT and the runout are also investigated.

4.2 *Surface generation modelling and experiment verification*

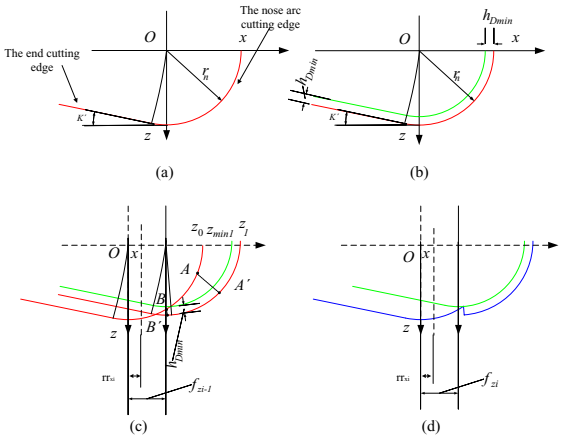

Fig. 6. The 2D surface generation modelling process

The details of the 2D surface generation model proposed in this paper are listed as followed. In Fig. 6a), by considering the analysed 2D plane along the centreline of the slot floor, the local coordinate system $x - z$ is defined. In Fig. 6b), the green line representing the MCT line is introduced. The MCT h_{Dmin} is determined by the normal distance between the profile of the cutter and the corresponding MCT line. Fig. 6c) shows that 2D surface generation process after the first tooth pass. The red line represents the tool profile at starting position. With each pass of the tool, the 2D surface profile can be formed by combining the previous surface profile. The micro-milling process in Fig. 6c) is one case for the first tooth pass. For example, in Fig. 6c), the normal distance AA' between the point A in the red line of starting position and point A' in the red line of the first tooth pass position is the cutting thickness which exceeds the MCT h_{Dmin}. Therefore, the chips are formed and the new 2D surface topography is renewed to include the point A'. While the MCT h_{Dmin} is larger than the cutting thickness which can be determined as normal distance between the point B in the red line of starting position and point B' in the red line of the first tooth pass position. Consequently, there is no chip formed and the new profile can be updated to include the point B'. Fig. 6d) illustrates the machined surface profile. The blue line represents the new surface generation after the first tooth pass, which is the machined surface profile.

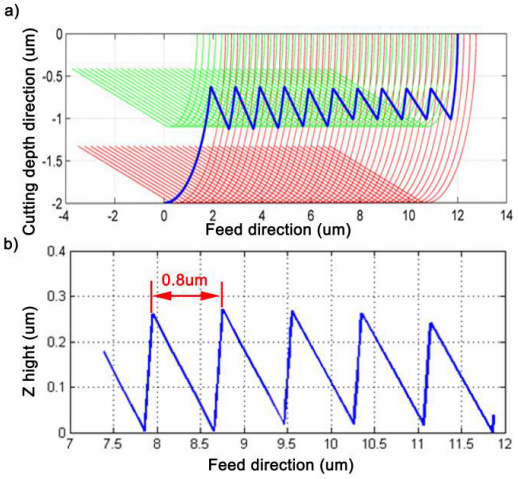

Fig.7 Simulation results with 0.2μm/tooth feed without tool runout. (a) cutter profile paths; (b) Zoomed-in view of machined surface profile

Fig.7a) shows the case when feed per tooth f_z = 0.2 μm/tooth which is less than MCT. It can be found that the chip is only formed when the uncut chip thickness is larger than the MCT, the interaction happens after four engagements, which means that there is no material removed by the first three engagements. Fig.7b) shows that the period of the surface profile is 0.8μm which is four times of f_z.

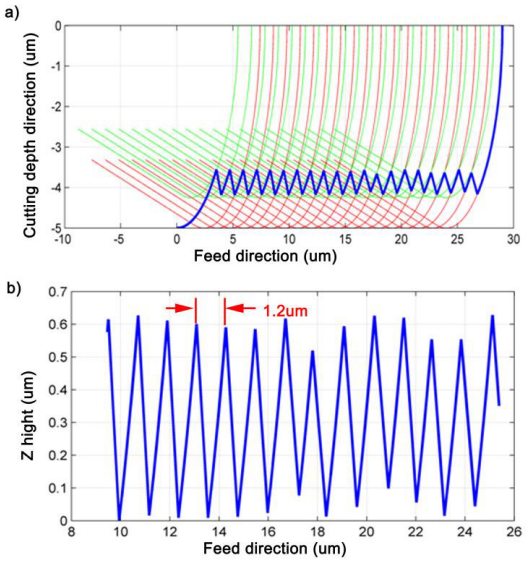

Fig.8 Simulation result with 1μm tool runout and 0.2μm/tooth feed, (a) cutter profile paths; (b) Zoomed-in view of machined surface profile

However, in the actual processing, tool runout is inevitable. Fig.8a) shows the trajectories of the tool path and its corresponding h_{min}.The f_z in this simulation was still selected as 0.2 μm/tooth, and the runout was set as 1μm. It is observed that in this case only one tooth participates in cutting, and the other tooth cut no material due to the runout. Fig.8b) shows the period of the surface profile is 1.2 μm, which is equal to the runout plus the feed per tooth.

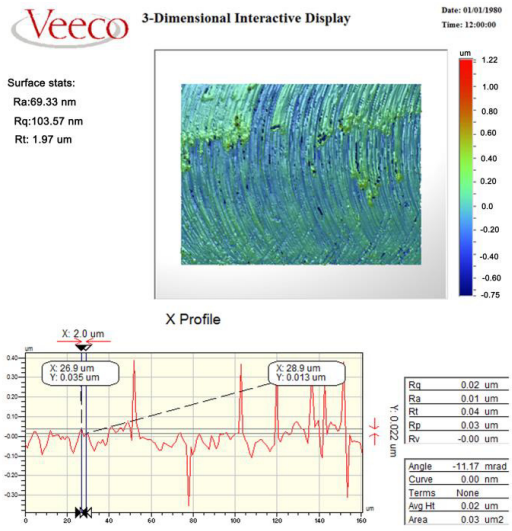

Fig.9 Surface measurement results with 1μm tool runout and 0.2μm/tooth feedrate

Full slot milling experiments on AISI 1045 steel were performed using the cutting parameters which are same as those in the simulation. Fig. 9 illustrates the surface measurement results, which is obtained from the white light interferometric surface profiler (Vecco NTll00). It can be found that the material removal takes place even when the feed per tooth is less than the MCT, which demonstrates the credibility of the proposed simulation model when feed per tooth is smaller than the MCT.

In order to verify the effectiveness of the proposed simulation model with large feed per tooth, another simulation was carried out with 6μm/tooth.

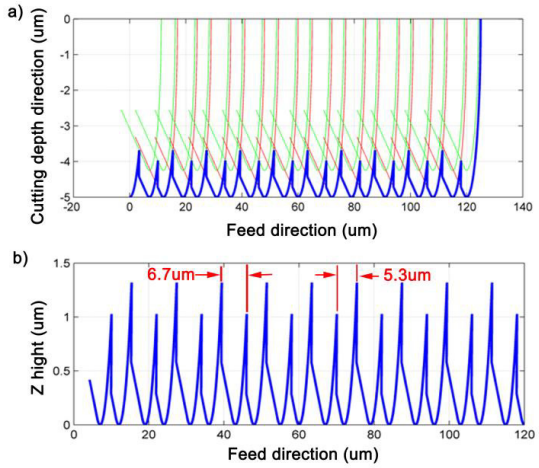

Fig.10 The simulation result with 1μm tool runout and 6μm/tooth, (a) cutter profile paths; (b) Zoomed-in view of machined surface profile

The effect of tool runout on the machined surface is clearly observed in Fig. 10 which shows the unevenness profile of the surface height. In a single tool revolution, the maximum chip thickness of the material removed by one tooth is larger than the value of feed per tooth but the other tooth is smaller than it. ,

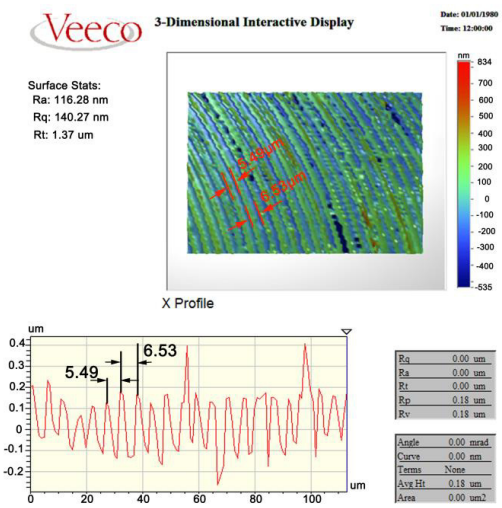

Fig.11 Surface measurement results with 1μm tool runout and 6μm/tooth feed

Fig. 11 shows the measurement results on the surface machined with 1μm tool runout and 6μm/tooth feed. Unevenness profile was observed, which agrees well with the simulation results in Fig.8. This demonstrates that the proposed simulation model is still effective even at large feed per tooth.

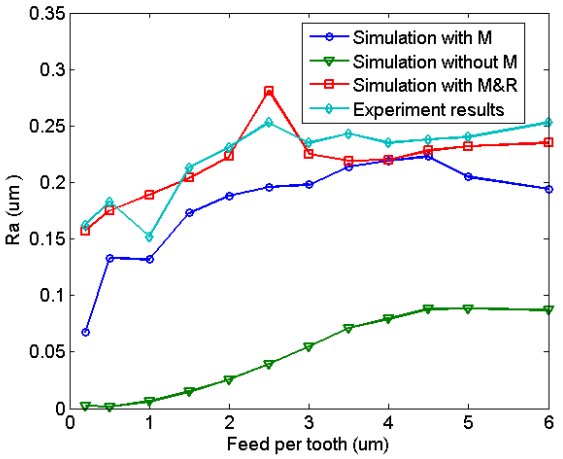

Fig.12 Comparisons of the predicted surface roughness and the experimental results

Fig. 12 shows the trends of surface roughness with the increase of the feed per tooth. Three prediction results, namely, without considering MCT and tool runout (Simulation without M), considering MCT only (Simulation with M), and both considering MCT and tool runout (Simulation with M & R), are presented in the figure together with experimental results. It can be found that the surface roughness increases with the increase of feed per tooth, and the surface roughness values are much smaller than the experimental results without considering the MCT and tool

runout. The surface roughness predictions are close to the experimental results when considering MCT, but it is still less than the experiment results. The predicted results from the proposed model considering both MCT and tool runout has a high prediction accuracy over a wide range of feedrate.

5 Conclusions

In this paper, a surface generation model for micro-end-milling has been developed by considering minimum chip thickness and tool runout in the machining process. A numerical model based on the trajectory and cutter geometry of micro-end mills was established, which can be used to describe the generation of machined surface profile and to estimate the surface roughness during the micro-end milling process. The simulation results were verified by micro milling experiments. The following conclusions can be drawn:

1) Due to tool runout, the material removal takes place even when the feed per tooth is less than the MCT.
2) In micro milling process, tool runout results in a significant increase of surface roughness, especially when the feed per tooth is less than the runout.
3) It is difficult to obtain a good surface roughness in small feed per tooth due to the presence of tool runout and the effect of minimum chip thickness.
4) The proposed surface generation model considering the minimum chip thickness and tool runout is more accurate in surface topography simulation and roughness prediction in micro milling.

Acknowledgements

The authors gratefully acknowledge financial support of the National Natural Science Foundation of China (Grant No.51505107), Natural Scientific Research Innovation Foundation in Harbin Institute of Technology (HIT.NSRIF.2017029) and the Engineering and Physical Sciences Research Council (EP/M020657/1).

References

[1] Cheng K, Huo D. Micro cutting: fundamentals and applications. Wiley, Chichester, 2013.
[2] Alting L, Kimura F, Hansen H, et al. Micro Engineering. CIRP Annals – Manufacturing Technology 2003;52:635–657.
[3] Huo, D., Lin, C., Choong, Z., Pancholi, K. and Degenaar, P. Surface and subsurface characterisation in micro-milling of monocrystalline silicon. International Journal of Advanced Manufacturing Technology, 2015; 81(5-8): 1319-1331.
[4] Andersson H, Van A. Microfluidic devices for cellomics: a review. Sensors and Actuators B: Chemical; 2003; 92: 315-325.
[5] Bang Y, Lee K, Oh S. 5-axis micro milling machine for machining micro parts. The International Journal of Advanced Manufacturing Technology 2005; 25: 888-894.
[6] Melkote S, Kumar M, Hashimoto F, et al. Laser assisted micro-milling of hard-to-machine materials. CIRP Annals-Manufacturing Technology 2009; 58: 45-48.
[7] Suzuki H, Moriwaki T, Yamamoto Y, et al. Precision cutting of aspherical ceramic molds with micro PCD milling tool. CIRP Annals-Manufacturing Technology 2007; 56: 131-134.
[8] Huo D, Cheng K, Wardle F. Design of a five-axis ultra-precision micro-milling machine—UltraMill. Part I: holistic design approach, design considerations and specifications. The International Journal of Advanced Manufacturing Technology 2010; 47: 867-877.
[9] Dhanorker A, Ozel T. Meso/micro scale milling for micro-manufacturing. International Journal of Mechatronics and Manufacturing Systems 2008; 1: 23-42.
[10] Oliaei S, Karpat Y. Experimental investigations on micro milling of Stavax stainless steel. Procedia CIRP 2014;14: 377-382.
[11] Bissacco G, Hansen H N, De Chiffre L. Size effects on surface generation in micro milling of hardened tool steel. CIRP Annals-Manufacturing Technology 2006; 55: 593-596.
[12] Saklakoglu I, Kasman S. Investigation of micro-milling process parameters for surface roughness and milling depth. The International Journal of Advanced Manufacturing Technology 2011; 54: 567-578.
[13] Sun Y, Liang Y, Du R. Simulation and analysis of surface generation in micro-milling. Proceedings of the 6th WSEAS International Conference on Robotics, Control and Manufacturing Technology, Hangzhou, China. 2006: 30-35.
[14] Yuan Z J, Zhou M and Dong S. Effect of diamond tool sharpness on minimum cutting thickness and cutting surface integrity in ultraprecision machining. J. Mater. Process. Technol 1996; 62:327–30
[15] Li H, Lai X, Li C, et al. Modelling and experimental analysis of the effects of tool wear, minimum chip thickness and micro tool geometry on the surface roughness in micro-end-milling. Journal of Micromechanics and Microengineering, 2007;18: 025006.
[16] Bao W, Tansel I. Modeling micro-end-milling operations. Part II: tool run-out. International Journal of Machine Tools & Manufacture 2000;40: 2175–2192.
[17] Simoneau A, Ng E, Elbestawi M. Grain size and orientation effects when microcutting AISI 1045 steel. CIRP Annals-Manufacturing Technology 2007; 56: 57-60.
[18] Son SM, Lim H, Ahn J. Effects of the friction coefficient on the minimum cutting thickness in micro cutting. International Journal of Machine Tools and Manufacture 2005;45: 529-535.
[19] Vogler M, Devor R, Kapoor S. On the modeling and analysis of machining performance in micro-endmilling, part I: Surface generation. Journal of Manufacturing Science and Engineering 2004;126:685-694.
[20] Ramos A, Autenrieth H, Strauss T, et al. Characterization of the transition from ploughing to cutting in micro machining and evaluation of the minimum thickness of cut. Journal of Materials Processing Technology 2012; 212: 594-600.
[21] Kang I, Kim J, Seo Y. Investigation of cutting force behaviour considering the effect of cutting edge radius in the micro-scale milling of AISI 1045 steel. Proceedings of the Institution of Mechanical Engineers, Part B: Journal of Engineering Manufacture 2011; 225:163-171.
[22] Huo, D. and Cheng, K. Experimental investigation on micromilling of oxygen-free, high-conductivity copper using tungsten carbide, chemistry vapour deposition, and single-crystal diamond micro tools. Proceedings of the Institution of Mechanical Engineers, Part B: Journal of Engineering Manufacture, 2010, 224: 995-1003.